Atmos. Meas. Tech. Discuss., 2, 2403–2422, 2009
www.atmos-meas-tech-discuss.net/2/2403/2009/

Atmospheric Measurement Techniques Discussions

Atmospheric Measurement Techniques Discussions is the access reviewed discussion forum of *Atmospheric Measurement Techniques*

Development of a bioaerosol single particle detector (BIO IN) for the fast ice nucleus chamber FINCH

U. Bundke[1], B. Reimann[1], B. Nillius[1], R. Jaenicke[2], and H. Bingemer[1]

[1]Institute for Atmospheric and Environmental Sciences, Goethe University, Frankfurt, Germany
[2]Institute for Physics of the Atmosphere, Johannes Gutenberg-University, Mainz, Germany

Received: 10 September 2009 – Accepted: 17 September 2009 – Published: 6 October 2009

Correspondence to: U. Bundke (bundke@iau.uni-frankfurt.de)

Published by Copernicus Publications on behalf of the European Geosciences Union.

Abstract

In this work we present the setup and first tests of our new BIO IN detector. This detector is designed to classify atmospheric ice nuclei (IN) for their biological content. Biological material is identified via its auto-fluorescence (intrinsic fluorescence) after irradiation with UV radiation. Ice nuclei are key substances for precipitation development via the Bergeron–Findeisen process. The level of scientific knowledge regarding origin and climatology (temporal and spatial distribution) of IN is very low. Some biological material is known to be active as IN even at relatively high temperatures of up to −2°C (e.g. *pseudomonas syringae* bacteria). These biological IN could have a strong influence on the formation of clouds and precipitation. We have designed the new BIO IN sensor to analyze the abundance of IN of biological origin. The instrument will be flown on one of the first missions of the new German research aircraft "HALO" (High Altitude and LOng Range).

1 Introduction

Ambient aerosol originates from multiple sources and consists of a wide variety of materials like mineral dust, sea salt, acids, soot, organic polymers, plant debris, pollen, bacteria and spores. Several recent publications focus on the sources, distribution and potential impact of aerosol particles of biological origin on atmospheric processes (Ariya and Amyot, 2004; Deguillaume et al., 2008; Georgakopoulos et al., 2009; Möhler et al., 2007, 2008; Morris et al., 2008; Pratt et al., 2009; Prenni et al., 2009; Szyrmer and Zawadzki, 1997). Biological particles have the ability to act as cloud condensation nuclei (CCN) and as ice nuclei (IN) in heterogeneous freezing processes even at high temperatures (Jaenicke, 2005; Jaenicke et al., 2007). High temperature IN can be bacteria (Vali and Schnell, 1975; Vali et al., 1976; Schnell and Vali, 1976; Maki and Garvey, 1975; Maki et al., 1974), pollen (von Blohn et al., 2005; Diehl et al., 2001, 2002), fungal spores, etc. Secondary ice formation e.g. by mechanical fragmentation,

splintering during riming of ice particles (Hallet-Mossop process) and fragmentation of large droplets during freezing will multiply the number of ice crystals in clouds by up to a factor of 10 000 (Heymsfield and Mossop, 1984; Mossop, 1985; Pruppacher and Klett, 1996). Thus, even a small number of IN will have the potential to alter the microphysical structure of a cloud and play a key role in mid-latitude precipitation formation by the Bergeron–Findeisen process.

The interest in the detection of particles of biological origin in ambient aerosol has greatly increased during the last decade. A method to distinguish biological material from non-biological particles utilizes the detection of autofluorescence (intrinsic fluorescence) after irradiation with UV radiation (Seaver et al., 1999; Pan et al., 2003, 2009; Hairston et al., 1997). Ho et al. (2000) compared fluorescence (UV-APS) measurements to reference sampler data that provide culturable or living bio aerosol number concentrations. Biological matter consists of various different substances. Some of them are efficient fluorophores. For the excitation of autofluorescence of these substances, two UV excitation wavelength ranges are common: 260–280 nm and 340–380 nm.

a) Wavelength range 260–280 nm

Protein fluorescence is induced by absorption of radiation in this wavelength range. The aromatic side-chains of the amino acids tryptophan, tyrosine and phenylalanine are primarily responsible for the inherent fluorescence of proteins. Tryptophan is the main fluorophore among them, since both its molar absorptivity and the fluorescence quantum yield are typically several times higher as compared to the other amino acids. Therefore absorption spectra of proteins often resemble the absorption of tryptophan and their maxima are mostly located at about 275–280 nm (Wetlaufer, 1962). The corresponding protein fluorescence emission maxima vary with the protein-solvent environment and are typically located in the region around 330–350 nm (Demchenko, 1986). However this UV range was not selected for excitation because false counts caused by non- biological aromatic hydrocarbons will occur.

b) Wavelength range 340–380 nm

Apart from the proteins, there are several enzymatic co-factors present, which act as bio-fluorophores at longer absorption wavelengths, namely the reduced forms of the nicotinamide adenine dinucleotide (NADH (Coenzyme 1)) and derivatives (e.g. NADPH) and the flavins (e.g. Riboflavin (Vitamin B2)). Upon excitation by UV radiation of about 360 nm wavelength the fluorescence emission range is 400–550 nm (see Fig. 1). These substances are used for our BIO IN Detector.

2 Experimental setup

The single-particle fluorescence detector for the in situ measurement of biological ice nuclei is based on the optical detector of the Fast Ice Nucleus CHamber (FINCH), which has been previously described in detail (Bundke et al., 2008).

Briefly, in FINCH a sample flow of ambient aerosol is mixed with a warm and moist air flow as well as with a cold and dry flow in the mixing region of the instruments chamber, where IN particles are activated at well-defined freezing temperatures and supersaturations (see Fig. 2). The particles grow while flowing through the processing chamber of 1.35 m length. All ice particles pass a virtual impactor, which removes 90% of the gas flow, including non-activated aerosol particles and small water droplets. The optical detector, which discriminates water droplets from ice crystals, is mounted behind the 2 mm outlet of the impactor. Here, the different depolarization behavior of water and ice with respect to scattered circular polarized light is used by analyzing the P44/P11 ratio of the scattering matrix. The collimated beam of a 30 mW 635 nm cw diode laser (Stocker Yale Inc., Salem, New Hampshire, USA) passes a circular polarizer and is mildly focused to an elliptical spot of 2×1 mm, which crosses the gas stream at a right angle (see Figs. 3 and 4). Light which is backscattered by droplets and ice crystals is measured in the range of 100 up to 130° scattering angle. After a condenser lens a $\lambda/4$ retarder (quarter wave plate) converts the circular polarized light back into linear polarized light, which is either 45 or 135° polarized from the principal axis, depending on the direction of circular polarization. A beam splitting cube separates the

two components P_{RC} and P_{LC} of the linear polarized light. The signals P_{RC} and P_{LC} are detected separately with two photodiodes. It is possible to discriminate water droplets and ice crystals, by determining the normalized P_{44}/P_{11} ratio of the scattering matrix, which is given by Eq. (1) for this particular case (see Bundke et al., 2008, for details). The only modification in this section of the detector is an additional 600 nm long pass filter, which is placed between the quarter wave plate and the beam splitting cube in order to avoid miscounting by scattered UV and fluorescence light.

$$P_{44}/P_{11} = \frac{P_{RC} - P_{LC}}{P_{RC} + P_{LC}} \quad (1)$$

The UV source used for the excitation of the bioaerosol particles is a fiber-coupled high-power LED with 250 mW output at 365 nm, operating in cw mode (LEDMOD365, Omicron Laserage, Rodgau, Germany). The UV light passes a 1000 µm UV silica fiber and is focused by a aspheric two-lens collimation-focusing assembly to a spot of about 2 mm diameter, which overlaps with both the 2 mm diameter cross section of the gas stream and the spot of the circular polarized 635 nm scattering laser (see Fig. 3). An 360 nm bandpass-emission filter (10 nm half-width) is positioned behind the lenses.

The fluorescence light is collected rectangular to the UV beam axis by an aspheric condenser lens and an additional spherical reflector. Two filters (long-pass 400 nm, short-pass 600 nm) separate the fluorescence light from the scattered light of both light sources. After this a second lens focuses it to a photomultiplier (H9656-20, Hamamatsu Photonics K.K., Iwata City, Japan, max. frequency bandwidth 200 kHz). Additionally a photodiode sensor is mounted behind a 400 nm short pass-filter, and a focusing lens in the forward scattering direction (35°) normalizes the signals to the intensity of the UV LED.

The signals are sampled in parallel by using a NI PCI 6132 data acquisition module with up to 3 MS/s per channel and are analyzed by a peak detection algorithm using the LabVIEW data acquisition software (National Instruments Corporation, Austin (TX), USA). While particles are detected using the circular depolarization detector,

bioaerosol particles are identified and counted, if the fluorescence signal extends a significant threshold value (5σ of the noise, see example signal Fig. 6). The ratio of the number of bioaerosol particles to the total number of particles is calculated.

3 Results

In this section we describe the initial laboratory tests of the newly developed sensor as well as a first probing of ambient aerosol.

3.1 Initial tests

Initial tests were performed on aerosol produced from a mixture of ca. 50% fluorescent 10 µm spherical silica particles ("Fluo-Blue", Spherotech, Lake Forest (IL), USA) and 50% non-fluorescent 10 µm spherical particles ("Silica particles", Spherotech, Lake Forest (IL), USA) in water suspension. The fluorescent dye has its excitation maximum at 350–360 nm, and the fluorescence emission wavelength ranges from 400 to 560 nm. Particles were suspended using a home-made atomizer and were dried by mixing with a dry carrier gas. The total gas flow was about 6 l/min, which is consistent with the flow rates of FINCH in normal operation mode. For the initial tests the detector was decoupled from FINCH, because silica particles are hardly IN active. Thus, using the complete FINCH setup did not make any sense (see Fig. 5 for details of the setup).

Figure 6 shows a snapshot of two particles passing the detector within one second. Here the photomultiplier was operated with a lower gain. The first (smaller) particle shows a significant fluorescence signal and the second particle almost no fluorescence signal.

In general the scattering intensities of the test particles were found to be relatively broadly distributed in the frequency histogram. However, a check of the aerosol size distribution using an aerodynamic particle sizer (APS, TSI Inc. type 3321) showed that our test aerosol was not monodisperse. The size distribution in front of the detector

was found to be similarly broad, with its maximum at about 8.5 µm.

The distribution of the fluorescence intensity seen in the related histogram of the frequency of occurrence was similarly broad, which can be explained with both the broad size distribution and the different dye concentrations in the silica particles. However, nearly 60% of the particles in the mixture showed fluorescence. This is consistent with the 50%/50% mixture of the fluorescing/non-fluorescing samples (within the large errors resulting from uncertainties of the concentrations of the two sample solutions and a fast sedimentation of the large particles).

3.2 Initial tests with ambient aerosol

Ambient aerosol was sampled directly through a 3 m×6 mm I.D. copper tube from the outside of the Geosciences Department building in Frankfurt am Main, Campus Riedberg, Germany, at 10 m above ground level on 26 June 2009, 14:30–16:10 LT. The sample flow rate was 5 l/min. A total number of 704 particles have been counted. 52 particles (6.3%) have been found to be clearly fluorescent and therefore of biological origin. This observed biological fraction of coarse mode particles is close to the 4%average value measured with a UV-APS (TSI Inc.) during a 4 month period (3 August–4 December 2006) at Mainz (Germany), close to Frankfurt (Huffman et al., 2009). A nine minute ambient sample taken with the APS directly after the BIO IN measurements resulted in a total number of 69 coarse particles larger than 3 µm. If one assumes that the particle concentration did not vary significantly during the time of both measurements, then we may conclude from the total counts that the BIO IN detector triggered particles larger than about 3 µm.

Figure 7 shows an example of a relatively small particle, for which the scattering intensity is only slightly above the triggering threshold, but which shows a strong fluorescence signal.

Figure 8 shows a scatter plot of the signal intensities in the scattering and the fluorescence channels. No correlation between particle size (proportional to the square root of the scattering intensity) and fluorescence intensity is observed. This is not surpris-

ing, given the large variance of biological particles in the atmosphere and the different concentrations of autofluorescent metabolites among them.

4 Conclusions

The new BIO IN detector constitutes an important contribution for the understanding of the origin of IN. It is known that some aerosol particles which contain biological material activate as IN at relatively high temperatures. They will thus activate first during cloud icing and will determine the temperature of the onset of cloud icing, and may alter the microphysical structure of the cloud significantly.

The performance of this low cost detector is better than we expected originally but is still limited because of the signal to noise ratio. Thus, the separation between biological and non-biological material is not sharp for particles with low fluorescence activity (e.g. spores). The fluorescence yield is related to the concentrations of NADH/NADPH and Flavoproteins (FAM, FAD, Riboflavin, etc.), which depend also on their oxidation state varying with the energy metabolism of the living cells. During our initial tests we identified at least 6% of coarse mode particles larger than 3 µm to be of biological origin.

5 Outlook

It is planned to enhance the signal to noise ratio by using a new 405 nm laser. Furthermore, we plan to test the setup with a powerful 355 nm solid state Laser, equivalent to the one used by the UV-APS of TSI company (Hairston et al., 1997). It may be possible then to differentiate various types of biological particles such as spores, pollen, bacteria, cell fragments, by use of a high speed spectrometer to obtain the dispersed fluorescence spectrum, instead of the simple photomultiplier. This will be the bestdesign possible – but not longer at low cost.

Another possible improvement is the use of photomultipliers in the scattering channels instead of the less sensitive photodiodes. By this one could expect to shift the detection limit to particle sizes smaller one µm.

The BIO IN detector as part of the FINCH measurement system is currently in the certification process for use onboard the new HALO aircraft.

Acknowledgements. We thank U. Pöschl for intensive discussions and suggestions and for providing the 4 Month period UV-APS time series at Mainz. This work has been performed within Project A1 of the Collaborative Research Centre (SFB) 641 "The Tropospheric Ice Phase", funded by the German Science Foundation and by the Grand Bu 1432/3-1 (Development of an ice nucleus (IN) counter for HALO) within the framework of SPP 1294: Atmospheric and Earth system research with the "High Altitude and Long Range Research Aircraft" and by the virtual institute Aerosol Cloud interaction VI233 funded by the Helmholtz society.

References

Ariya, P. A. and Amyot, M.: New directions: The role of bioaerosols in atmospheric chemistry and physics, Atmos. Environ., 38, 1231–1232, 2004.

Bundke, U., Nillius, B., Jaenicke, R., Wetter, T., Klein, H., and Bingemer, H.: The fast ice nucleus chamber FINCH, Atmos. Res., 90, 180–186, 2008.

Deguillaume, L., Leriche, M., Amato, P., Ariya, P. A., Delort, A.-M., Pöschl, U., Chaumerliac, N., Bauer, H., Flossmann, A. I., and Morris, C. E.: Microbiology and atmospheric processes: chemical interactions of primary biological aerosols, Biogeosciences, 5, 1073–1084, 2008, http://www.biogeosciences.net/5/1073/2008/.

Demchenko, A. P.: Ultraviolet Spectroscopy of Proteins, Springer, Berlin, London, p. 312, 1986.

Diehl, K., Quick, C., Matthias-Maser, S., Mitra, S. K., and Jaenicke, R.: The ice nucleating ability of pollen: Part I: Laboratory studies in deposition and condensation freezing modes, Atmos. Res., 58, 75–87, 2001.

Diehl, K., Matthias-Maser, S., Jaenicke, R., and Mitra, S. K.: The ice nucleating ability of pollen: Part II. Laboratory studies in immersion and contact freezing modes, Atmos. Res., 61, 125–133, 2002.

Georgakopoulos, D. G., Després, V., Fröhlich-Nowoisky, J., Psenner, R., Ariya, P. A., Pósfai, M., Ahern, H. E., Moffett, B. F., and Hill, T. C. J.: Microbiology and atmospheric processes: biological, physical and chemical characterization of aerosol particles, Biogeosciences, 6, 721–737, 2009, http://www.biogeosciences.net/6/721/2009/.

Hairston, P. P., Ho, J., and Quant, F. R.: Design of an instrument for real-time detection of bioaerosols using simultaneous measurement of particle aerodynamic size and intrinsic fluorescence, J. Aerosol Sci., 28, 471–482, 1997.

Heymsfield, A. J. and Mossop, S. C.: Temperature-dependence of secondary ice crystal production during soft hail growth by riming, Q. J. Roy. Meteor. Soc., 110, 765–770, 1984.

Ho, J., Spence, M., and Hairston, P.: Measurement of biological aerosol with a fluorescent aerodynamic particle sizer (FLAPS): Correlation of optical data with biological data, Rapid Meth. Anal. Biol. Mater. Environ,, 30, 177–201, 2000.

Huffman, J. A., Treutlein, B., and Pöschl, U.: Fluorescent biological aerosol particle concentrations and size distributions measured with an ultraviolet aerodynamic particle sizer (UV-APS) in Central Europe, Atmos. Chem. Phys. Discuss., 9, 17705–17751, 2009, http://www.atmos-chem-phys-discuss.net/9/17705/2009/.

Jaenicke, R.: Abundance of cellular material and proteins in the atmosphere, Science, 308, 73–73, 2005.

Jaenicke, R., Matthias-Maser, S., and Gruber, S.: Omnipresence of biological material in the atmosphere, Environ. Chem., 4, 217–220, 2007.

Maki, L. R., Galyan, E. L., Changchi. M., and Caldwell, D. R.: Ice nucleation induced by pseudomonas-syringae, Appl. Microbiol., 28, 456–459, 1974.

Maki, L. R. and Garvey, D. M.: Bacterially induced ice nucleation, Trans. Am. Geophys. Union, 56, 994–994, 1975.

Möhler, O., DeMott, P. J., Vali, G., and Levin, Z.: Microbiology and atmospheric processes: the role of biological particles in cloud physics, Biogeosciences, 4, 1059–1071, 2007, http://www.biogeosciences.net/4/1059/2007/.

Möhler, O., Georgakopoulos, D. G., Morris, C. E., Benz, S., Ebert, V., Hunsmann, S., Saathoff, H., Schnaiter, M., and Wagner, R.: Heterogeneous ice nucleation activity of bacteria: new laboratory experiments at simulated cloud conditions, Biogeosciences, 5, 1425–1435, 2008, http://www.biogeosciences.net/5/1425/2008/.

Mossop, S. C.: Secondary ice particle-production during rime growth – the effect of drop size distribution and rimer velocity, Q. J. Roy. Meteor. Soc., 111, 1113–1124, 1985.

Palumbo, G. and Pratesi, R.: Lasers and Current Optical Techniques in Biology, Royal Society of Chemistry, Cambridge, xxiv, p. 658, 2004.

Pan, Y. L., Hartings, J., Pinnick, R. G., Hill, S. C., Halverson, J., and Chang, R. K.: Single-particle fluorescence spectrometer for ambient aerosols, Aerosol Sci. Technol., 37, 628–639, 2003.

Pan, Y. L., Pinnick, R. G., Hill, S. C., and Chang, R. K.: Particle-fluorescence spectrometer for real-time single-particle measurements of atmospheric organic carbon and biological aerosol, Environ. Sci. Technol., 43, 429–434, 2009.

Pratt, K. A., DeMott, P. J., French, J. R., Wang, Z., Westphal, D. L., Heymsfield, A. J., Twohy, C. H., Prenni, A. J., and Prather, K. A.: In situ detection of biological particles in cloud ice-crystals, Nature Geosci., 2, 397–400, 2009.

Prenni, A. J., Petters, M. D., Kreidenweis, S. M., Heald, C. L., Martin, S. T., Artaxo, P., Garland, R. M., Wollny, A. G., and Poschl, U.: Relative roles of biogenic emissions and Saharan dust as ice nuclei in the Amazon basin, Nature Geosci., 2, 401–404, 2009.

Pruppacher, H. R. and Klett, J. D.: Microphysics of Clouds and Precipitation, 2nd rev. and engl. edn., vol. 18, Atmospheric and Oceanographic Sciences library, Kluwer Academic Publishers, Boston, xx, 954 pp., 1996.

Schnell, R. C. and Vali, G.: Biogenic ice nuclei. 1. Terrestrial and marine sources, J. Atmos. Sci., 33, 1554–1564, 1976.

Seaver, M., Eversole, J. D., Hardgrove, J. J., Cary, W. K., and Roselle, D. C.: Size and fluorescence measurements for field detection of biological aerosols, Aerosol Sci. Technol., 30, 174–185, 1999.

Szyrmer, W. and Zawadzki, I.: Biogenic and anthropogenic sources of ice-forming nuclei: A review, B. Am. Meteorol. Soc., 78, 209–228, 1997.

Vali, G. and Schnell, R. C.: Biogenic sources of atmospheric ice nuclei – review, Trans. Am. Geophys. Union, 56, 994–994, 1975.

Vali, G., Christensen, M., Fresh, R. W., Galyan, E. L., Maki, L. R., and Schnell, R. C.: Biogenic ice nuclei. 2. Bacterial sources, J. Atmos. Sci., 33, 1565–1570, 1976.

von Blohn, N., Mitra, S. K., Diehl, K., and Borrmann, S.: The ice nucleating ability of pollen: Part III: New laboratory studies in immersion and contact freezing modes including more pollen types, Atmos. Res., 78, 182–189, 2005.

Wetlaufer, D. B.: Ultraviolet spectra of proteins and amino acids, Adv. Protein Chem., 17, 303–390, 1962.

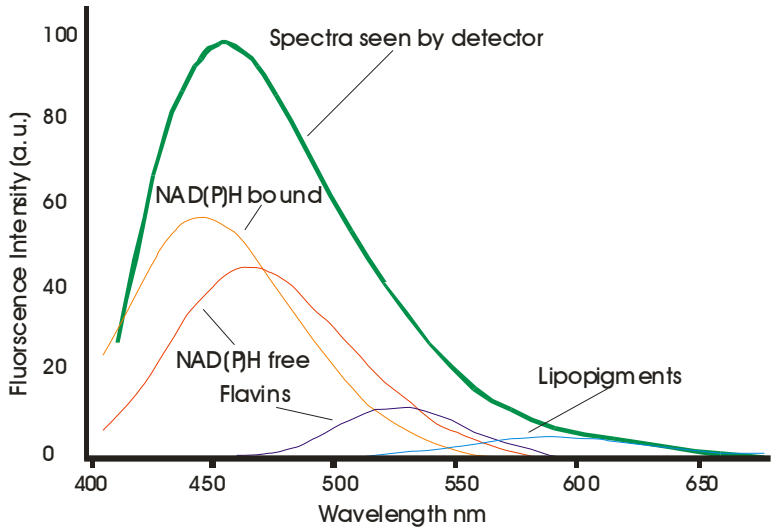

Fig. 1. Scheme of autofluorescence emission spectra of NADH, Flavins and Lipopigments. The sum of the different emission spectra in the 400–600 nm range will give the signal strength measured by the BIO IN detector. Figure modified from (Palumbo and Pratesi, 2004).

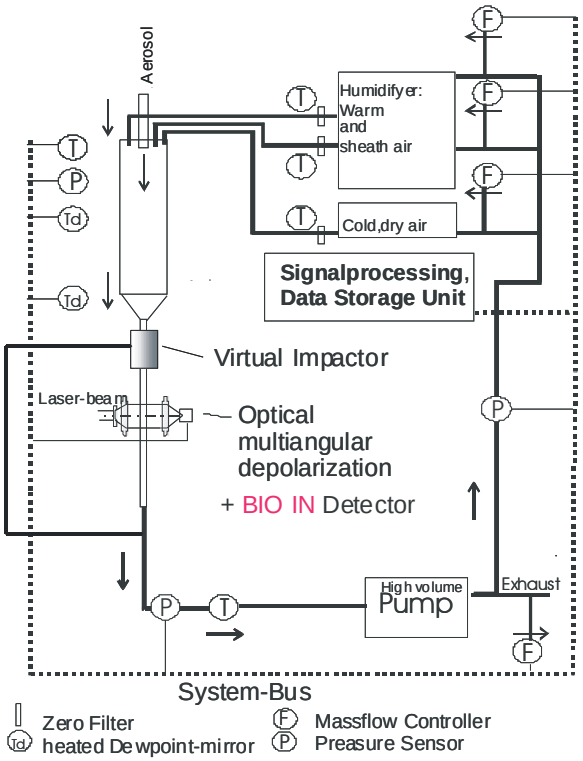

Fig. 2. Schematic flow diagram of the FINCH counter. The new Bio IN detector is incorporated in the depolarization detector located behind the virtual impactor at the bottom of the development section. Modified from (Bundke et al., 2008).

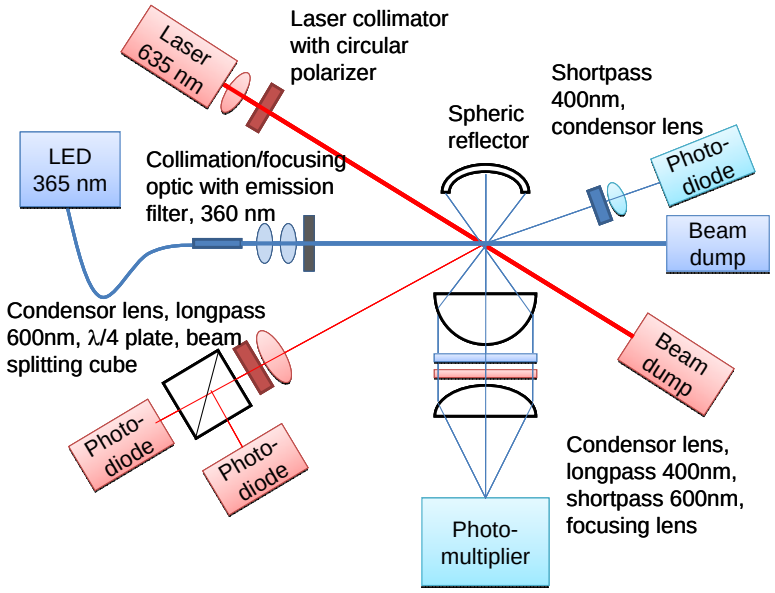

Fig. 3. Schematic diagram of the Bio IN detector optics. The aerosol flow intersects the paper plane vertically at the point of intersection of the laser and UV-LED beam (see also Fig. 4).

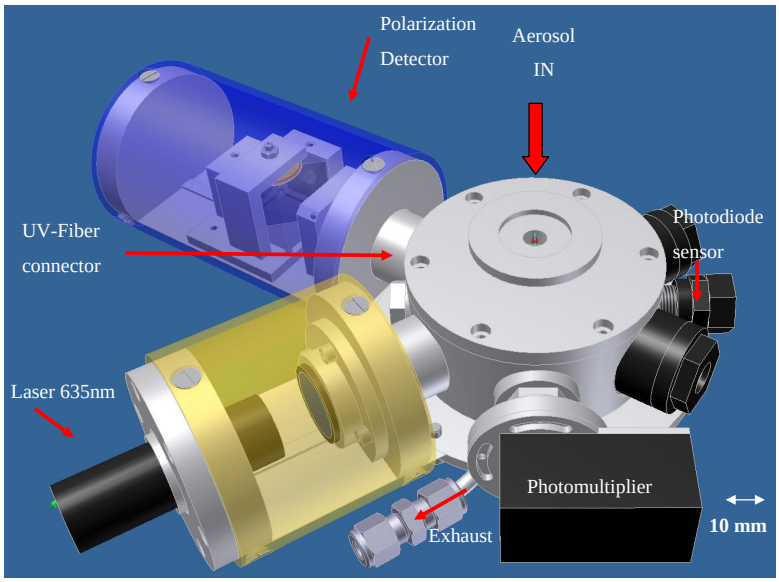

Fig. 4. Physical setup of the BIO-IN detector.

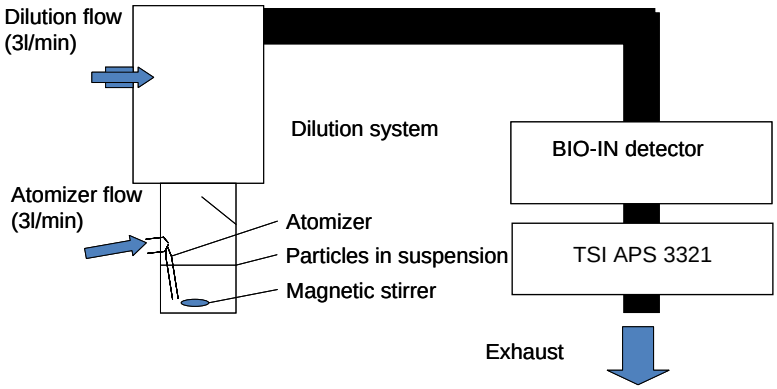

Fig. 5. Schematic diagram of the test-aerosol suspension unit (silica microsphere particles, see text for details).

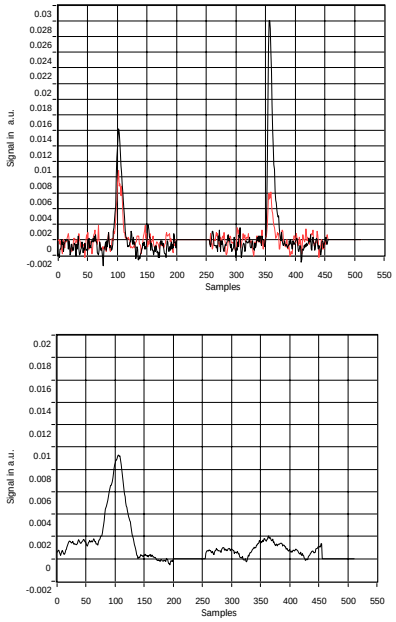

Fig. 6. Example of a snapshot where two test particles have passed the detector within one second. On the y-axis the signal voltage and on the x-axis the sample number taken at 200 kHz are shown. The signal was triggered, thus peaks are centered at sample number 100. If more than one particle was detected the signal was added with a gap of 56 samples in advance. The upper panel shows the phase discriminating depolarization channel (P_{RC} red line and P_{LC} black line), the lower the flourescence channel. Particles are counted as fluorescent if the signal maximum is larger than $5\sigma_{\text{noise}}$. For this measurement σ_{noise} is 0.0006 V which corresponds to a detection limit of 0.003 V. In this example the first particle shows a significant but weak flourescence signal. The second particle shows no or only an extremely weak fluorescence and is therefore counted as non-fluorescent. The signals in the fluorescence channel are generally broader than the photodiode signals because the circular spot size of the UV source is larger than the elliptical spot of the diode laser. Thus the particles need more time to travel through the detection volume.

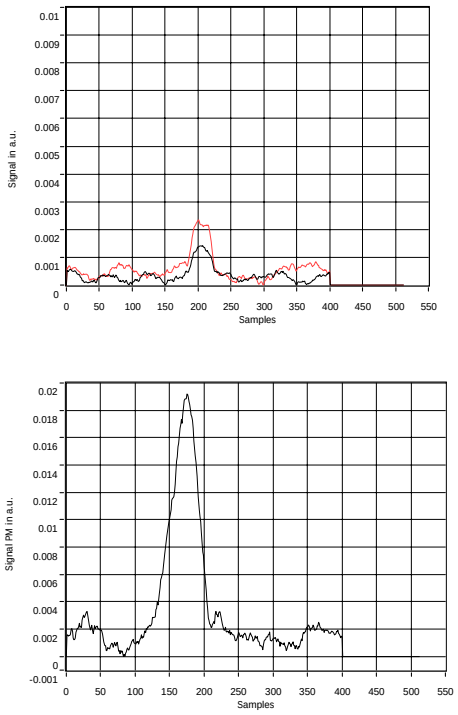

Fig. 7. Example of a snapshot where one small ambient particle have passed the detector.On the y-axis the signal in V and on the X-axis the sample number taken at 200 kHz are shown. The signal was triggered, thus peaks are centered at sample number 200. The upper panel shows the phase discriminating depolarization chanel, the lower panel shows the fluorescence channel. In this case a small particle (weak scattering signal) exhibits a strong fluorescence signal. Here it is obvious that particle size is not directly correlated to the fluorescence signal (see also Fig. 8). The small shift of the signal maxima of about 25 samples (=100 μs) between the two channels originates from a small misalignment of the two beams.

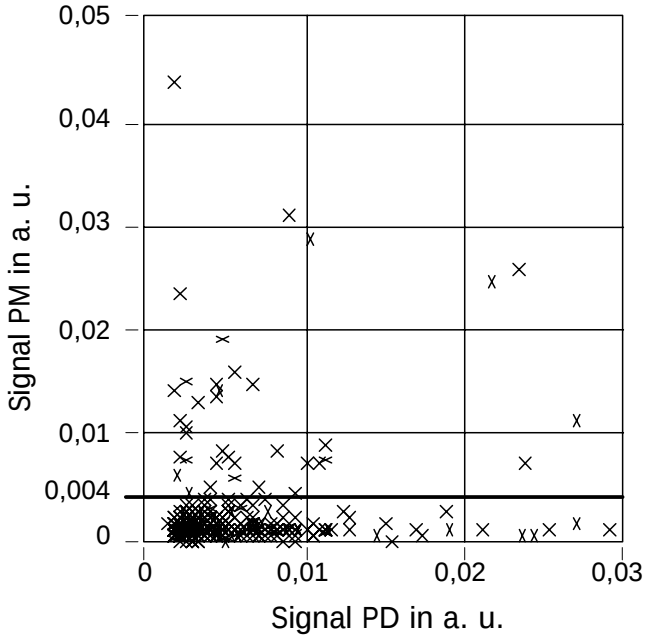

Fig. 8. Scatter plot of the fluorescence signal versus the scatter signal intensity on the basis of single particle analysis. There is no significant correlation between particle size (scatter intensity) and fluorescence signal strength.